$a-b$ Anisotropy of the Intra-Unit-Cell Magnetic Order in $YBa_2Cu_3O_{6.6}$

Lucile Mangin-Thro,[1,*] Yuan Li,[2,†] Yvan Sidis,[1] and Philippe Bourges[1]
[1]*Laboratoire Léon Brillouin, CEA-CNRS, Université Paris-Saclay, CEA Saclay, 91191 Gif-sur-Yvette, France*
[2]*Max Planck Institute for Solid State Research, 70569 Stuttgart, Germany*
(Received 18 October 2016; published 2 March 2017)

Within the complex phase diagram of the hole-doped cuprates, seizing the nature of the mysterious pseudogap phase is essential for unraveling the microscopic origin of high-temperature superconductivity. Below the pseudogap temperature $T^\star$, evidence for intra-unit-cell orders breaking the fourfold rotation symmetry have been provided by neutron diffraction and scanning tunneling spectroscopy. Using polarized neutron diffraction on a detwinned $YBa_2Cu_3O_{6.6}$ sample, we here report a distinct $a-b$ anisotropy of the intra-unit-cell magnetic structure factor below $T^\star$, highlighting that intra-unit-cell order in this material breaks the mirror symmetry of the CuO_2 bilayers. This is likely to originate from a crisscrossed arrangement of loop currents within the CuO_2 bilayer, resulting in a bilayer mean toroidal axis along the **b** direction.

DOI: 10.1103/PhysRevLett.118.097003

Upon doping with charge carriers, the lamellar copper oxides evolve from antiferromagnetic Mott insulators to high-temperature superconductors. On the underdoped side of their phase diagram [Fig. 1(a)], hole-doped cuprates exhibit unusual electronic and magnetic properties in the so-called pseudogap (PG) phase below $T^\star$ [1]. Among cuprate families, various studies in $YBa_2Cu_3O_{6+x}$ (YBCO) have enabled researchers to obtain a particularly deep understanding of the PG phase. This bilayer system, the structure of which is shown in Fig. 1(b), becomes weakly orthorhombic owing to the formation of CuO chains upon increasing oxygen stoichiometry from $x=0$ to 1, but the CuO_2 layers are commonly believed to retain a nearly tetragonal structure that leaves room for spontaneous breaking of the C_4 rotational symmetry (into C_2) in the electronic and/or magnetic structure. As a strain field, the weak orthorhombicity can facilitate observation of such symmetry breaking by eliminating one of the two possible domains, yielding an $a-b$ anisotropy of physical properties that is much more pronounced than the structural orthorhombicity itself. Such an anisotropy has been reported in electrical transport [2], spin dynamics [3–5], the Nernst coefficient [6,7], and nuclear magnetic resonance [8] measured on detwinned single crystals. In the PG state of another bilayer cuprate $Bi_2Sr_2CaCu_2O_{8+\delta}$ [9], scanning tunneling microscopy also highlighted an intra-unit-cell (IUC) electronic nematic state with unbalanced electronic density on oxygen sites along **a** and **b**.

The breaking of time reversal symmetry (TRS) is another feature of PG physics. Indeed, an IUC magnetic order develops below a temperature $T_{\rm mag}$, matching $T^\star$, as reported by polarized neutron diffraction in four cuprate families [10–18]. In YBCO, this order is long ranged at low doping [11,14], becomes short-ranged around optimal doping [19], and vanishes at high doping. This IUC magnetic order indicates that translation invariance is preserved, but TRS is broken in the PG state. In addition, resonant ultrasound measurements reported a weak anomaly at $T^\star$, indicating that the PG phase is a true broken symmetry state [20]. Recently, optical second-harmonic generation

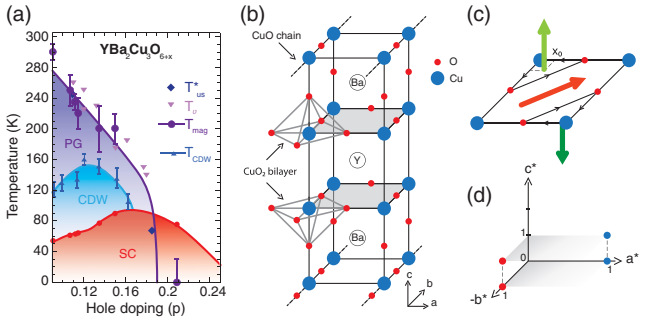

FIG. 1. $YBa_2Cu_3O_{6+x}$ phase diagram and structure, and the loop currents as a possible model for the cuprates. (a) $YBa_2Cu_3O_{6+x}$ phase diagram as a function of hole doping (p), showing the PG, the incipient charge density wave (CDW) and superconducting (SC) phases. The following values are reported: $T^\star_{\rm us}$ from resonant ultrasound measurements [20], $T_{\rm mag}$, the temperature of the magnetic IUC order [16,19], T_ν, the onset of $a-b$ anisotropy from the Nernst effect [6], and $T_{\rm CDW}$, the onset of CDW correlations from resonant x-ray measurements [34]. (b) Crystal structure of the bilayer compound $YBa_2Cu_3O_{6+x}$ with the CuO chains running along **b**. (c) Loop current model [25,26]: each loop induces an orbital magnetic moment $\mathbf{M_i}$ (green arrows) perpendicular to the CuO_2 plaquette, located at the triangle center, $x_0=0.146$. The red arrow represents the associated anapole or toroidal moment $\mathbf{T}\simeq\sum_{\mathbf{i}}\mathbf{M_i}\times\mathbf{r_i}$ ($\mathbf{r_i}$ stands for the vector connecting the center of the unit cell and the location of the ith moment). (d) Location of the studied magnetic Bragg reflections: wave vectors, given in reduced lattice units, of the form of $\mathbf{Q}=(1,0,L)$ (blue circles) and $\mathbf{Q}=(0,1,L)$ (red circles) have been studied.

measurements in YBCO have further reported a global broken inversion symmetry at $T^\star$ [21], confirming that the pseudogap region coincides with a hidden order. Among other theoretical proposals [22–24], the most consistent interpretation of the IUC magnetism [19] remains the loop current (LC) model for the PG state [25–27]. It is found to coexist with electronic nematic order [28] as well as charge-density wave states [29,30]. The most promising type of LC pattern consists of two counterpropagating LCs flowing over copper and neighboring oxygen sites within each CuO_2 unit cell, producing a pair of out-of-plane staggered orbital magnetic moments ($\mathbf{M_i} = \pm\mathbf{M}$) separated along a given diagonal [Fig. 1(c)]. For a single CuO_2 layer, four degenerate LC patterns exist, identified by their toroidal moment or anapole [26] $\mathbf{T} = \sum_\mathbf{i} \mathbf{r_i} \times \mathbf{M_i}$ [red arrow in Fig. 1(c)] along the other diagonal, along which the inversion symmetry is also broken. The associated IUC magnetic structure factor probed by neutron diffraction can, therefore, be anisotropic along both diagonals, but no $a-b$ anisotropy is expected as far as a single CuO_2 layer is concerned.

Motivated by the fact that in underdoped YBCO for a hole doping larger than $p \sim 0.1$, both the $a-b$ anisotropy in the Nernst coefficient [6] and the IUC magnetic order are set below $T^\star$ [Fig. 1(a)], we have carried out a polarized neutron diffraction in a detwinned YBCO sample. We observe an $a-b$ anisotropy in the IUC magnetic structure factor with distinct magnetic intensities along $\mathbf{a}^*$ and $\mathbf{b}^*$ which show that the mirror symmetry of the CuO_2 bilayers is broken below $T^\star$. Our data can be described by a crisscrossed arrangement of loop currents within the CuO_2 bilayer, with a resulting toroidal axis along the CuO chain, **b**, direction.

We here report polarized neutron measurements on a low-doped $YBa_2Cu_3O_{6.6}$ ($T_c = 63K$, $p = 0.12$) detwinned single crystal, previously used to study spin dynamics [3]. The polarized neutron experiments have been performed on the triple-axis spectrometer 4F1 (Orphée, CEA-Saclay). A polarizing supermirror (bender) and a Mezei flipper are inserted on the incoming neutron beam in order to select neutrons with a given spin. In addition, a filter (pyrolytic graphite) is put before the bender to remove high harmonics. After the sample, the final polarization, **P**, is analyzed by a Heusler analyzer. The incident and final neutron wave vector are set to $k_I = k_F = 2.57$ Å^{-1}. Following previous studies [10–19], the search for magnetic order in the pseudogap phase is performed on Bragg reflections $\mathbf{Q} = (1,0,L)/(0,1,L)$ with integer $L = 0, 1$ values. The general methods to extract the IUC magnetic signal have been discussed in Refs. [10–19], and the important steps for our analysis are reported in the Supplemental Material [31].

In order to compare the magnetic signals along the directions $\mathbf{a}^\star = [1,0]$ [blue symbols in Fig. 1(d)] and $\mathbf{b}^\star = [0,1]$ (red symbols), measurements were carried out at Bragg reflections of the form of $\mathbf{Q} = (1,0,L)/(0,1,L)$ with $L = 0$ or $L = 1$ in reciprocal lattice units. Here, we focus on the scattered magnetic intensity for two neutron spin polarizations **P** (see the Supplemental Material [31]): (i) $\mathbf{P}\|\mathbf{Q}$, which measures the full magnetic scattering intensity and (ii) $\mathbf{P}\perp\mathbf{Q}$ in the scattering plane, where predominantly the out-of-plane magnetic component, $\mathbf{M_c}$, is probed.

Figure 2 shows the raw neutron intensity on two Bragg peaks along the directions $\mathbf{a}^\star$ and $\mathbf{b}^\star$ for $L = 0$ and $\mathbf{P}\|\mathbf{Q}$. The intensities for two neutron spin states are shown in the spin-flip (SF) channel, when the scattering process flips the neutron spin at the sample position, and the non-spin-flip (NSF) channel, when it is preserved. Following a standard procedure [10–12,14–16,19], both curves have been normalized at high temperature over some temperature range (here between 250 and 330 K). On the one hand, NSF intensity represents the nuclear Bragg peak intensity which exhibits a continuous decay when increasing the temperature as expected for a Debye-Waller factor. As the sample is detwinned, the NSF intensity along $\mathbf{b}^\star$ [Fig. 2(b)] is weaker than along $\mathbf{a}^\star$ [Fig. 2(a)]. On the other hand, the SF scattering intensity probes a true SF magnetic scattering (if any) on top of a polarization leakage of the NSF channel into the SF channel. The latter is given by the NSF intensity divided by the flipping ratio FR^0. For a perfectly spin-polarized neutron beam, FR^0 goes to infinity and the leakage vanishes. On top of the normalized nuclear scattering, the SF intensity then exhibits an extra scattering at low temperature that is attributed to the IUC magnetic component (Fig. 2). In both the $\mathbf{a}^\star$ and $\mathbf{b}^\star$ directions, the magnetic signal appears below $T_{\mathrm{mag}} \sim 240$ K, in agreement with $T_{\mathrm{mag}} = 220\ \mathrm{K} \pm 20\ \mathrm{K}$ determined in an early study on the same sample matching $T^\star \sim 230$ K deduced from

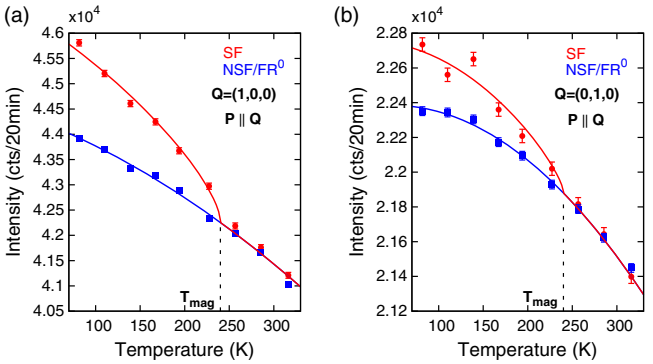

FIG. 2. Raw Bragg peaks intensity. Temperature dependence of the spin-flip (SF) (red circles) and non-spin-flip (NSF) (blue squares) neutron intensity for a neutron polarization $\mathbf{P}\|\mathbf{Q}$. (a) At $\mathbf{Q} = (1,0,0)$ (along $\mathbf{a}^\star$). (b) At $\mathbf{Q} = (0,1,0)$ (along $\mathbf{b}^\star$). In the SF channel, a magnetic signal is observed below $T_{\mathrm{mag}} \sim 240$ K on top of the NSF intensity normalized at high temperature by a constant flipping ratio, $FR^0 \sim 40$. Data have been averaged over a temperature range of 25 K to improve the statistics. Error bars of standard deviation are about the size of the points.